Impacts of the baking heating rate on the water mobility, starch microstructure and mechanical properties of degassed crumb during staling

Roua Bou Orm, Vanessa Jury, Xavier Falourd, Lionel Boillereaux, Luc Guihard, Alain Le-Bail

Impacts of the Baking Heating Rate on the Water Mobility, Starch Microstructure and Mechanical Properties of Degassed Crumb During Staling

Roua BOU-ORM[ab d], Vanessa JURY[abd], Xavier FALOURD[c d], Lionel BOILLEREAUX[ab d], Luc GUIHARD[abd], Alain LE-BAIL[ab d]

[a] ONIRIS, BP 82225, 44322 Nantes– France

[b] UMR GEPEA CNRS 6144 - ONIRIS, 44307 Nantes – France

[c] UR 1268 Biopolymères Interactions Assemblages, INRA, 44316, Nantes, France

[d] SFR IBSM 4402, 44316, Nantes, France

***Corresponding author: alain.lebail@oniris-nantes.fr**

Abstract

In this study, the impacts of different heating rates (HRs) from 6 to 40°C/min were investigated in terms of the ^{1}H proton water mobility, starch microstructure, texture, soluble amylose (AM), amylopectin (AP) retrogradation and AM crystallization during staling. A degassed breadcrumb baked in a miniaturized baking system was used to ensure better time-temperature control during baking. Proton nuclear magnetic resonance (^{1}H NMR) data showed that the evolution of the proton T_2 relaxation time decreased with increasing HR during staling. The amount of soluble AM, AP retrogradation degree, AM crystallization degree and crumb firmness tend to increase at higher HR. Environmental scanning electron microscopy (ESEM) observations showed that most starch granules in crumbs treated at higher HR exhibited strong deformation and disruption. These results confirmed that the increase in crumb firmness during staling with increasing HR was related to a higher level of starch disruption. This yielded a higher degree of separation between the AM and AP, which resulted in more pronounced water trapping in the starch crystals. The resulting dehydration

of the matrix (gluten network, with AM gel surrounding of starch granules) yielded a loss in crumb softness, and crumb baked at higher HR tended to have a firmer texture and faster staling.

Keywords: Staling, heating rate, AP retrogradation, AM crystallization, ^{1}H NMR mobility, firmness.

Abbreviations: Heating rate (HR), amylose (AM), amylopectin (AP), proton nuclear magnetic resonance (^{1}H NMR), Environmental scanning electron microscopy (ESEM), conventional baking (CVB), Young's modulus (E), dry flour (d.f.).

1. Introduction

Different parameters related to the baking process, such as the baking temperature, heating rate (HR), baking duration and temperature beyond the gelatinization temperature affect the texture and staling rate of bread. The HR potentially affects access to water and therefore the swelling of starch granules and the amount of leached amylose (AM) (Besbes et al., 2014). Hence, the HR may influence the evolution of the firmness during staling (Besbes et al., 2014; Palav and Seetharaman, 2007). Besbes et al., (2016) studied the effect of two HRs on bread staling corresponding to the case of conventional baking (CVB) at 4.67°C/min and 6.31°C/min for oven temperatures of 220°C and 240°C, respectively. It was observed that a higher HR resulted in a higher moisture loss and an increased crumb firmness. Furthermore, Patel et al., (2005) investigated the effect of two HRs in CVB at 16.8°C/min and 6°C/min with different dough piece sizes. These authors found that staling was more pronounced at higher HRs (Patel and Seetharaman, 2006). AM crystallization seemed to be affected by the HR, and this parameter could be considered to monitor crumb staling and the crumb texture, as reported in previous literature. In addition, the HR affects the availability of water and the degree of starch granule disruption during baking, which affect the staling parameters.

The aim of this study was to assess the impact of the HR on bread crumb staling. Compared with the existing literature, this study considers a large range of HRs (6°C/min, 20°C/min and 40°C/min) obtained by using a miniaturized baking system to allow the baking of degassed bread crumb. The properties of the crumb were evaluated to monitor different parameters related to the progression of staling, including the texture, AP retrogradation and AM crystallization (Chinachoti et al., 2013; Ribotta and Le Bail, 2007). Water mobility was assessed by low field NMR (Curti et al., 2017, 2013, 2011; Engelsen et al., 2001), and environmental scanning electron microscopy was used to examine the extent of starch granule disruption (Roman-Gutierrez et al., 2002). In addition to the large HR range tested, there is a novel focus on the amount of AM complexes formed during baking as a function of the HR with AM crystallization, the amount of soluble AM and water molecular mobility to investigate the impacts of the HR on starch granule disruption during baking.

2. Material and methods:

2.1. Raw materials

The white flour (Giraudineau, Saint-Colomban, France) used for the formulation had the following properties: 12% water, 10% protein, 1.4% total fat, 64.5% enzymatic starch, and 0.6% ash with a falling number of 450 s. The Alveograph parameters (Chopin Technologies, Villneuve, France) were as follows: Deformation energy (W: 373.10^4J), Ratio Tenacity/Extensibility (P/L: 1.48). The recipe was composed as follows: 100 g of flour, 51.43 g of water, 4.43 g of compressed yeast (l'Hirondelle, Marquette-lez-Lille, France), 1.8 g of salt (Esco, Levallois-Perret, France), 3.03 g of rapeseed oil, 7.83 g of sugar (Saint Louis, Paris, France), 1.72 g of improvers (Wheat gluten and alpha-amylases,) purchased from Puratos, Rungis,France and 0.507 g of emulsifier (Mono and diglycerides of rapseed fatty acid) and Xanthan gums (Cargill, Saint Nazaire, France).

73 **2.2. Bread-making procedure**

74 A batch of 500 g of ingredients was mixed in an alveograph mixer (Chopin Technologies,
75 Villneuve, France) for 7 min at 60 rpm (final temperature of 30°C). The dough was allowed to
76 rest for 5 min, divided and molded manually to obtain dough pieces that were 30 g each. The
77 dough pieces were placed in a fermentation cabinet (Hengel, Parigny, France) with a relative
78 humidity of 80% for 90 min at 38°C. The dough expansion ratio at the end of fermentation
79 was 3.5, corresponding to a conventional fermentation process. After being fermented, the
80 dough was placed in a plastic pouch, which was placed in a vacuum sealer machine (Maxima
81 Kitchen Equipement, Mijdrecht, Holland). Vacuum was applied for 1 min to remove all pores
82 in the dough before the pouch was sealed. The pouch was flattened and installed in a
83 miniature baking system composed of two Peltier elements (5 cm x 5 cm) (Le-Bail et al.,
84 2009). The thickness and the parallelism of the dough sample were controlled by a metallic
85 spacer (4 cm × 4 cm × 3 mm) located between the two Peltier elements. Three HRs were
86 applied, namely, 6°C/min, 20°C/min or 40°C/min, until a baking plateau was reached at 98°C,
87 which was held for 2 min (98°C is the plateau temperature of bread crumb during baking in
88 conventional conditions), followed by cooling to 20°C in 10 min. At the end of the baking
89 process, the samples were equilibrated for 40 min in a temperature-controlled cabinet at 20°C
90 (Memmert, Schwabach, Germany). The degassed crumb samples were detached from the
91 plastic pouch; disks of degassed baked crumb of 5 mm diameter were obtained using a
92 cylindrical cutter and stored in Eppendorf tubes at 4°C in a temperature-controlled cabinet
93 (Memmert, Schwabach, Germany) for 14 days. The baked crumb samples were analyzed for
94 moisture content, firmness, AP and AM crystallization and soluble AM after 2 h and 1, 3, 7,
95 and 10 days of storage.

96 **2.3. Moisture content (MC)**

97 The MC was determined according to the AACC method 44-15A (AACC, 1999). Two
98 grams of bread samples were weighed in aluminum cups using a precision scale with a 1-mg
99 resolution (SCALETECH, Argenteuil, France) and then dried in an oven (Memmert,
100 Schwabach, Germany) at 103°C for 24 h. Once it was returned to room temperature using a
101 desiccator, the dry sample was weighed again. The resulting difference in weight represents
102 the quantity of water initially present in the bread sample, expressed in g/100 g dm (dry
103 matter) units. Measurements were conducted in four replicates.

104 **2.4. Mechanical Properties**

$$Stress\ (\sigma) = F / S \qquad (1)$$

$$\textit{Strain } (\varepsilon) = \Delta L / L_0 \quad (2)$$

105 The crumb texture was evaluated using a dynamic mechanical analyzer (DMA Q800-
106 TA-Waters instruments-78-Guyancourt-France) to perform compression tests on the degassed
107 bread crumb baked in the Peltier cooker. Two parallel cylinders of 2cm diameter were used to
108 compress the degassed crumb disks (5mm diameter and 3 mm height) at room temperature
109 20°C. A static force of 0.02 N was used to start the test and to establish contact between the
110 parallel cylinders and the sample. The cylinders were slightly lubricated with a piece of tissue
111 containing rapeseed oil. Each sample of the degassed crumb was exposed to compression at a
112 rate of 5% per minute up to 30% deformation. The graph of the stress with respect to the
113 strain was plotted. The stress (σ) and strain (ε) were calculated using equations (1) and (2),
114 respectively. Considering the stress as a function of the strain, the corresponding Young's
115 modulus (E) was calculated based on the slope of the linear part of the curve between -0.5%
116 and -8% and expressed in N/mm² or MPa (Le-Bail et al., 2009). Compression tests were
117 performed after 2 h and 1, 3, 6 and 10 days of storage to study the evolution of the texture
118 during staling.

119 Where F is the static force expressed in N, S is the sample surface area in mm^2, ΔL is
120 the change in length in mm and L_0 is the initial length in mm

121 **2.5. Calorimetry Analysis**

122 Two different calorimeters were used to monitor the phase changes of the starch and
123 starch components after baking. The degree of starch gelatinization and amount of retrograded
124 AP during storage were studied with micro DSC VII equipment (SETARAM Instrumentation,
125 Lyon, France), and the degree of AM crystallization was investigated with a TA-Q100
126 calorimeter (TA Q1000, TA Instruments, New Castle, US-DE). The SETARAM calorimeter
127 has a very high sensitivity but was unable to reach the high temperature needed to analyze the
128 AM complexes (done with TA-Q100). A sample of 100 mg to 200 mg of crumb was taken

129 from the degassed crumb slab and placed in a hermetical cell (TA Instruments, New Castle,
130 US-DE).

131 A Denver balance with 0.01 mg accuracy (Denver Instruments CO., Arvada, US-CO) was
132 used for weight measurement. The analysis procedure was as follows. After equilibrating the
133 sample at 20°C for 5 min, a temperature increase was programmed up to 120°C with a
134 scanning rate of 1.2°C/min. The enthalpies of transition (the melting enthalpy of retrograded
135 AP starting at approximately 40°C and starch gelatinizationat 60-70°C) were obtained by
136 integrating each peak found in the thermogram and were expressed in units of J/g dry flour.
137 The degree of starch gelatinization allows for the quantification of nongelatinized starch; this
138 may occur, particularly in the case of rapid heating and/or a lack of water. The endotherm
139 linked to starch gelatinization starts at approximately 60°C in excess water (80% water
140 content, no restriction to water access) (Silverio et al.,1996). The excess water was evaluated
141 from the dry matter content of the considered product based on the dry matter of the crumb
142 (dry matter was determined by drying tests performed in a drying cabinet at 103°C for 24 h
143 according to the AACC method 44-15A, AACC, 1999). The degree of gelatinization was

$$\textbf{Degree of gelatinization} = \left(\mathbf{1} - \frac{\textbf{Gelatinization enthalphy of the bread sample}}{\textbf{Gelatinization enthalphy of dough}}\right) \boldsymbol{X}\mathbf{100}\% \qquad \textbf{(3)}$$

144 estimated according to the equation (3) (Ding et al., 2019):

145 The melting enthalpy of AM-lipid complexes and AM crystallization (from approximately
146 90/100°C until the end of the endotherm peak) were determined using a Q100 calorimeter
147 (TA Q100, TA Instruments, New Castle, US-DE). The calorimeter (TA Q100) was
148 programmed up to 180°C with a scanning rate of 3°C/min; these tests were performed to
149 monitor and quantify the evolution of the AM crystallized during storage. The associated
150 enthalpy was determined by integrating the surface of the peak with Universal-ANALYSIS

151 software (TA Instruments, version 4.5A). Measurements were performed in triplicate for
152 bread baked at different HRs and stored for each storage durations.

153 **2.6. Determination of soluble amylose**

154 Determination of soluble AM permits the evaluation of the degree of starch disruption
155 during baking. The AM leached from the starch granules is dispersed into the matrix and
156 contributes to the final cohesiveness and texture of the crumb. The AM gel formed during
157 storage is expected to play a significant role in the mechanical properties of the texture of the
158 crumb, even though most authors indicated that AP recrystallization is the main driver. The
159 amount of soluble AM was measured according to the AACC 61-03 method. One hundred
160 milligrams of baked crumb was stirred in 100 ml of a solution (10% ethanol - 65% v/v, 9%
161 NaOH 1 N and 81% desalinated water) to evaluate the amount of soluble AM and total AM.
162 After stirring, the sample was left at room temperature for 18 h (total AM) or 2 h (soluble
163 AM); 150 µl was sampled after the extraction period and was diluted in a solution containing
164 60 µl of Lugol, 30 µl of acetic acid (1 N) and 1.5 µl of desalinated water. The solution was
165 stirred and left for 20 min to rest. The absorbance at 620 nm was determined with a
166 spectrophotometer (CM 3500-d, Konica Minolta Sensing Inc., Mahwah, US-NJ). Tests were
167 performed in triplicate for each sample using three 3-ml flasks for each storage duration
168 because the amount of soluble amylose is known to decrease with increasing storage time due
169 to the more pronounced organization of the retrograded AM (Patel et al., 2005). Calibration
170 was performed with a blank and with a sample containing 27% pure AM (Corn starch, Argo,
171 Best Food, CPC International Inc., Bergen, US-NJ). The percentage of AM was calculated
172 from the absorbance of the sample multiplied by 27 and divided by the absorbance of the
173 reference sample (27%). Three repetitions were performed for each data point.

174 **2.7. Nuclear magnetic resonance (NMR) measurements**

For each HR, NMR tests were performed for samples stored at 4°C for 24 h, 6 days and 14 days after baking. First, 0.5 g of crumb samples (diameter (Ø) = 8 mm and height (H) = 10 mm) was placed in an NMR tube closed with a cap (Ø = 10 mm). Then, the tube of each sample was placed in the spectrometer and thermostatically maintained at 277 K. NMR analysis was carried out using a Minispec mq20 spectrometer (Bruker, Milton, Burlington, Canada).). The transverse T_2 relaxation time of protons as well as their respective population in the product was determined using a Carr–Purcell–Meiboom–Gill (CPMG) sequence. The 180° pulse separation was 0.075 ms, 1000 even echoes were collected, and 512 scans were acquired with a recycle delay of 2 s, resulting in a total acquisition time of approximately 20 min. An inverse Laplace transformation (ILT) was applied to convert the relaxation signal into a continuous distribution of T_2 relaxation times. The T_2 distributions were then deconvoluted, and each "peak" was modeled using an asymmetric normal law (Berman et al., 2010). The software used was developed (in part) and implemented using MATLAB©R2014a (MathWorks, Natick, US-MA).

2.8. Environmental Scanning Electronic Microscopy Images

Environmental Scanning Electronic Microscopy (ESEM) is an electron microscopy technique (Philips, Leuven, Belgium) capable of producing high-resolution surface images. ESEM scans the surface of the sample to be analysed with an electron beam to obtain data at the particle scale. Different detectors that reconstruct a three-dimensional image of the surface were used to analyze these particles. The crumb samples, stored at 4°C, were fractured into sizes of approximately 1x1x0.5 cm using a knife and a hammer before the sample was quickly transferred to the SEM chamber. The interior surface of the samples was coated with an ultrathin coating of metal (gold) or carbon. A 2D image of the sample was displayed on a computer monitor. The crumb samples were scanned by a focused electron beam in a Philips XL30-ESEM system at an accelerating potential of 8 kV at 4°C. Secondary electrons were

processed to form enlarged images with a magnification of 500 X. Scans of samples were realized under the following conditions in the SEM chamber: a vapor pressure of 660 Pa and a temperature of 4°C.

2.9. Staling kinetics

The evolution of the melting enthalpy of AP and AM as a function of the storage time was modeled according to the Avrami equation (first-order kinetic models) by assuming that the time exponent was equal to unity (Le-Bail et al., 2012; Le-Bail et al., 2009). The Avrami equation was used to model the evolution of the melting enthalpy of AP $\Delta \boldsymbol{H}$ (t) (**equation (4)**) with $\Delta \boldsymbol{H_0}$ and $\Delta \boldsymbol{H}_\infty$ representing the melting enthalpy at initial and final times, respectively, where τ is the time constant and *t* is the storage time (in days). A similar equation was used to model the crumb hardening (from the Young's modulus E (t)) of the degassed breadcrumb (**equation (5)**) with $\boldsymbol{E_0}$ and $\boldsymbol{E}_\infty$ corresponding to the Young's modulus at the initial and final times, respectively.

$$\Delta \boldsymbol{H(t)} = \Delta \boldsymbol{H}_\infty + (\Delta \boldsymbol{H_0} - \Delta \boldsymbol{H}_\infty)\boldsymbol{exp}(-\boldsymbol{t}/\boldsymbol{\tau}) \quad \textbf{(4)}$$

$$\boldsymbol{E(t)} = \boldsymbol{E}_\infty + (\boldsymbol{E_0} - \boldsymbol{E}_\infty)\boldsymbol{exp}(-\boldsymbol{t}/\boldsymbol{\tau}) \quad \textbf{(5)}$$

Fitting the model and the experimental points was performed using Excel Solver (EXCELSTAT-Microsoft, Las Vegas, US-NV).

2.10. Statistical analysis

All experiments were performed in triplicate, and values were expressed as the mean ± standard deviation (SD). Statistical analyses were conducted using Statgraphics plus 5.1 software (Statgraphics Technologies, The Plains, US-VA) Fisher's Least Significant Difference (LSD) test was used to compare the means at the 5% significance level.

3. Results and discussion

3.1. Young's Modulus (E)

Fig. 1A shows the evolution of the firmness of the baked crumb samples during storage according to the variation in the E. The results demonstrate that the firmness of the breadcrumbs increased significantly ($p<0.005$) for all samples during storage. However, some differences occurred depending on the baking conditions. It was observed that E was lower after 2h storage for bread baked at 6°C/min (long baking and lower heating rate; 0.45 MPa) than for bread baked rapidly at 20°C/min (0.65 MPa) and 40°C/min (0.9 MPa). Indeed, the lowest value of E obtained at the end of staling (after 14 days storage) was 0.85 MPa for bread baked at 6°C/min while the highest Young's modulus at $t\infty$ was 2 MPa and corresponded to bread baked at 40°C/min.

Bredariol et al., (2019) also reported a significant correlation between heating rate and crumb hardness (for bread baked without steam). These authors observed that breadcrumb hardness tended to increase with increasing heating rate. In addition, Shen et al., (2018)noticed that the bread samples prepared with different types of sugar (the same sugar concentration) had the highest crumb firmness when higher baking temperatures for the same baking time (higher heating rate) were applied. These results could be explained by the fact that the heating rate during baking affects starch properties, including starch gelatinization (swelling and dispersion), amylose solubility, and amylopectin recrystallization (Tao et al., 2020). Therefore, these properties may have an influence on the evolution of crumb firmness during storage (Patel et al., 2005).

3.2. Evolution of AP recrystallization

Amylopectin retrogradation is one of the biochemical phenomena most closely associated with staling. Many authors have correlated this parameter with both bread crumb firmness and storage time (Ribotta, Cuffini et al., 2004). The degree of AP recrystallization was found to

increase during storage and was higher in samples baked at higher HRs (**Fig. 1B**). On 1 of storage, the AP recrystallization enthalpy was higher in crumb samples baked at higher HRs (0.38 J/g d.f. for 20°C/min and 0.5 J/g d.f. for 40°C/min) than in those baked at 6°C/min (0.15 J/g d.f.). After 10 days'storage, the AP recrystallization enthalpies increased for all HRs. The final enthalpy at the end of AP retrogradation was more important for the 40°C/min (1.8 J/g d.f.) than for the 20°C/min and 6°C/min HRs. Hence, the HR may affect the extent of the disordering of the AP crystals and the destructuring of starch. It is assumed that the higher amount of leached AM yields a higher degree of segregation between AM and AP (Tao et al., 2020).

The AP chains were organized in specific domains, resulting in the faster recrystallization of AP during storage of samples baked with high HRs, even from the first day of storage. Similar observations were reported by Patel and Seetharaman (2006). They confirmed that the enthalpy of recrystallized AP was higher in samples baked at higher HRs than in those baked at lower HRs. According to these results, the higher rigidity of the crumb samples could be associated with intramolecular dehydration of the crumb cell matrix du to the transfer of water molecules from gluten to AP crystallites. The capture of water by AP crystals no longer plasticizes the different networks. This can lead to an increase in crumb firmness and a decrease in crumb resilience, due to a less flexible gluten network (Goesaert et al., 2009, Ribotta and Le-Bail, 2007, Gray and Bemiller, 2003). Moreover, bread samples baked at a higher HR staled faster. This could be related to the higher capability of AP to retrograde at a higher HR (E. Besbes et al., 2014,).

3.3. Soluble amylose and amylose crystallization during storage

The soluble AM contents of the crumb samples were plotted as a function of the HR during storage (**Fig. 1C**). The amount of soluble AM decreased significantly after two days of staling for all the samples and continued to decrease slightly throughout the storage period.

Breads baked at higher HRs had higher soluble AM contents than bread crumb samples baked at lower HRs. After 2 h of storage, the crumb baked at 40°C/min had 8% soluble AM, crumbs baked at 20°C/min had 5.2% soluble AM and crumbs baked at 6°C/min had 4.7% soluble AM.

These results are in agreement with the hypothesis on AM leaching reported by Seyhun et al., 2005. They mentioned "the Higo effect" as a rapid change of AM when bread is baked at higher HR. This effect was explained by a considerable leaching of AM out of starch granules when bread is heated at a higher HR (40°C/min), as in microwave heating. The leached AM was found to be more disoriented during storage and more water molecules were bound to AM crystals (associations) than conventionally heated bread (6°C/min) (Seyhun et al., 2005). Moreover, during storage, the soluble AM decreased more in crumb samples baked at higher HRs than in those baked at lower HRs. After 10 days'storage, the soluble AM content decreased by 6.3%. 3.5% and 3.4% for bread baked at 40°C/min, 20°C/min and 6°C/min, respectively. The decrease in the soluble AM content during storage can be explained by the increase in AM molecule associations in their crystalline form. The latter increases during storage, as shown in **Fig. 1D**.

Fig. 1D shows the evolution of the AM associations (crystallized) as a function of the storage time. Such approaches appear novel, and so far there are no similar studies have been found in the literature. The amount of crystallized AM was found to increase with increasing HR. This was attributed to the increase in the concentration of soluble AM released from starch granules caused by a higher HR. After 10 days'storage, the crystallized AM enthalpies reached 4.3 J/g d.f. for an HR of 40°C/min, and 3.7 J/g d.f. and 3.2 J/g d.f. for bread baked at 20°C/min and 6°C/min, respectively. When baking at higher HR, the leached AM seemed to be more concentrated at the surface of starch granules, where the latter were richer in AP. Upon cooling and during storage, the surrounding AM molecules aligned into a crystalline

structure and formed a gel. This gelation induced the formation of ordered structures such as double helices during storage and the hardening of the crumb (Seyhun et al., 2003,Uzzan et al., 2007).Patel and Seetharaman (2006) reported that at higher HRs, AM leaching out of starch granules is rapidly associated with the surface of starch granules and/or phase separation from AP within the granules. These results confirm findings on the impact of the HR on the bread texture related to starch modification and concentrations.

3.4.Staling kinetics

The Avrami equation was developed to analyze the staling kinetics of starchy food such as bread (E. Besbes et al., 2014) and cake (Lee et al., 2020). The Avrami equation was used to model the evolution of crumb firmness and starch retrogradation during staling (Sang et al., 2015). Several authors have stated that for starch crystallization, the time exponent (n) is related to the crystal nucleation mechanism and growth with n varying between 1 and 4 (Mouneim et al., 2012; Rojas et al., 2001; Gujral et al., 2003). On the other hand, according to Le-Bail et al., (2009), the time exponent was equal to one for bread firming. For n=1, the time constant τ can be determined from the slope of the linear regression of the difference between the final value (long storage) and current value of the paremeters evaluated (Young's modulus and starch crystallization enthalpies) as a function of time. The slower the τ was, the higher the staling kinetics was.(E. Besbes et al., 2014; Lee et al., 2020). To fit the evolution of Young's modulus and the melting enthalpy of AP and AM crystallization (staling parameters) during storage a simple first order model (n=1) was used for this study (Equation 5 and 6). This model can fit very well with the experimental results for samples baked in a miniaturized baking system according to Mouneim et al., 2012 and Le-Bail et al., (2009).

Table 1 presents the parameters of the first-order model obtained from the model calculated by Excel-Solver (Excel-Solver, Microsoft USA) using an Avrami model. For the AP retrogradation model and AM crystallization, the value of the origin (time zero = day of

baking) was set to zero, which corresponds to the observed results in **Fig. 2**. At time zero, Young's Modulus was significantly higher at 40°C/min and 20°C/min and lower at 6°C/min.

At the end of storage, the enthalpy linked to AP retrogradation and AM crystallization increases with increasing HR. This trend was also observed for E (2 MPa at 40°C/min versus 0.85 MPa at 6°C/min), which refers to the evolution of crumb firmness. The time constant τ is presented in Table 1; as τ decreases, faster staling is observed. It was shown that the time constants of all the parameters (AM, AP and E) decreased with increasing HR. Using the first order kinetic model (Besbes et al 2014), this confirms that faster baking leads to faster staling. First, this trend explained by the reorganization and crystallization of AM and retrogradation of AP. These phenomena take more time with increasing HR due to the greater amount of crystallized material (as shown in **Fig. 1**). Second, the smaller values of the time constants obtained for E are followed by AM crystallization and AP retrogradation; the average values of the time constant were approximately 0.6, 1.05 and 3.48 days at 40°C/min.

In previous studies, most researchers found a direct relationship between the retrogradation of AP and the evolution of crumb firmness during staling. Kang et al., (2021) reported that the recrystallization of amylopectin is the main reason for samples staling during storage and bread firmness. Gray and Bemiller, (2003) reported similar observations. It was noted that starch retrogradation/recrystallisation, plays a major role in bread firming, after the initial cooling process. This was not the case in this study, as the increase in bread firmness appeared roughly at the same time as the increase in AM crystallization.Therefore, in this study using a specific recipe with low water content and improvers induced the formation of a large amount of AM complexes which can affect (restrict) the evolution of crumb firmness during storage, as discussed by Kang et al., (2021).

3.5. Starch swelling and microstructure

Starch granules morphology and the degree of gelatinization, is directly dependent on baking temperature, time and the resulting crumb firmness. **Fig. 2** illustrates ESEM images at 550 x magnification for the starch granules in bread crumbs baked in the Peltier system at different HRs. **Fig. 2A** shows that the starch granules in crumbs baked at 6°C/min had a regular, swollen elliptical shape with smooth surfaces in which the starch granules seemed to be completely gelatinized (with a degree of gelatinization of 100%, as indicated by a calorimetry study). Similar observations were reported by Ozkoc et al., (2009) for bread baked by conventional baking where the heating rate corresponded to 6°C/min. It was seen that starch granules observed by SEM were completely gelatinized and had a continuous starch granule structure.

In **Fig. 2B**, a HR of 20°C/min led to an increase in granule shape deformation with complete disruption and some superficial cracks. A large increase in HR (40°C/min) results in incomplete folding of starch granules, with the complete destruction and rupture of most of them (**Fig. 2C**). Additionally, the starch granules appeared to be nonhomogeneous and irregular, with many granular remnants. The starch underwent significantly less gelatinization at 40°C/min. The enthalpy of gelatinization associated with the nongelatinized starch in crumbs baked at 40°C/min was 0.65 J/g of dry flour, representing 80% of the gelatinized starch. Consequently, a higher HR will potentially alter the swelling kinetics and the disorganization of AP crystals and AM leaching. These changes can subsequently have an impact on the bread texture during storage (Kinner M. et al., 2021).The results obtained are in agreement with Bredariol et al., (2019) and Bilbao-Sáinz et al., (2007). These authors found that high heating rates lead to an increase in the enthalpy of gelatinization above the levels of native starch granules with a decrease in the gelatinization temperature. This is explained by the fact that starch granules are severely damaged when exposed to very high temperatures for

a short baking time (higher heating rate) and do not have enough time to complete its gelatinization.

3.6. Effect of the HR on the molecular water mobility and distribution of stored crumb

Measurement of the moisture content of degassed crumb (baked in a sealed pouch and stored in hermetically plastic Eppendorf tube) showed a nonsignificant difference for each HR and during staling. The limited changes in degassed crumb MC meant that changes in the proton distributions of the T_2 relaxation time during storage were exclusively attributed to changes in the starch and gluten networks (Bosmans et al., 2013; Curti et al., 2017, 2011). In our study, the T_2 relaxation time was measured by the CPMG sequence, and a continuous distribution is shown in **Fig. 3**. The continuous distribution permits us to characterize up to five proton populations and name them according to the length of their relaxation times A (0.3-0.5 ms), B (0.9-2.2 ms), C (3-10 ms), D (12-20 ms), and E (40-60 ms). The population abundance distribution was calculated and is represented in **Table 2**. P_{2A} and P_{2B} were the smallest populations, representing 3% of the total protons in baked degassed dough. Population C represents more than 80% of the total proton population, and D and E encompassed 7% of the total proton population. Moreover, our values of the T_2 relaxation time of different populations were reported in some studies where each population corresponded to a specific proton domain.

According to Engelsen et al. (2001), a relaxation time peaking at 0,5 ms (T_{2A}) corresponds to protons associated with water-gluten. Population B with a peak time of 2 ms is attributed to protons of intragranular water retained by starch (Assifaoui et al., 2006). Population C observed at 5.0 ms could probably be assigned to mobile protons of gluten and water associated with these molecules (Engelsen et al., 2001). Population D, ranging between 10 ms and 20 ms, is related to protons associated with gelatinized starch (and pentosane) (Curti et al., 2011; Engelsen et al., 2001) and corresponds to intergranular water, especially in interactions and competition with sucrose and starch (Assifaoui et al., 2006). Bosmans et al.,

(2014) reported that a relaxation time peak at 10 ms is associated with the mobile protons of water exchanging in the formed gel network (Bosmans et al., 2014). The T_{2E} of the last population, ranging from 50–60 ms, is related to the most mobile protons of water (less interacting with macromolecules) available in the aqueous phase of bread (Assifaoui et al., 2006; Rondeau-Mouro et al., 2019). The T_2 relaxation time and population abundance were affected by the HR and varied during storage. T_{2A} slightly decreased for the two higher HRs of 20°C/min and 40°C/min from 0.52 ms to 0.4 ms and increased for the lowest HR of 6°C/min from 0.44 ms to 0.53 ms following storage. Similarly, T_{2B} significantly decreased for the 2 higher HRs of 20°C/min and 40°C/min from 1.8 ms to 1.3 ms and 1.8 ms to 1.5 ms, respectively, and a slight but nonsignificant decrease was observed for 6°C/min. The relative amount of protons in populations A and B varied significantly at the higher HR after 14 days of storage, decreasing to 2.8% and increasing to 4.4% and varied insignificantly for samples baked at lower HRs.

Populations A and B might reflect the hydration state of the gluten network or the degree of gluten-water association. The decrease in their relaxation time is explained by the loss of water from the gluten network in bread and the migration of water from gluten to starch at higher HR. The slight increase in T_{2A} and the unchanged T_{2B} values upon storage for the 6°C/min rate might be attributed to the higher degree of gluten network hydration and the more plasticization that occured during storage and resulted in crumb firmness limitations (Bosmans et al., 2013; Curti et al., 2011). This decrease was also observed in the starch water model with 47% MC stored for up to 7 days, as reported by Bosmans et al. (2013). These authors suggested that in the gluten-starch model, dehydration of gluten occurs due to water migration from gluten during storage. The majority of detectable protons in population C decreased in abundance after 14 days of storage from 80% to 77% for the higher HR of 40°C/min, decreased from 84% to 80% for the 20°C/min HR and remained stable for the

6°C/min HR. The relaxation time slightly decreased for all HRs. In addition, the T_{2D} component decreased significantly after 14 days of storage from 15 ms to 13 ms for the 40°C/min HR and slightly decreased for the 20°C/min and 6°C/min HRs. The decreases in the relaxation time for components C and D upon storage could be due to the retrogradation of AP and the incorporation of water molecules in starch crystallites, which become less mobile at a higher HR. In contrast, at lower HRs, the crystallization phenomena are slower, which explains the slight decrease in T_{2C} and T_{2D}.

During storage, starch crystallization phenomena such as AP retrogradation and AM crystallization occur (particularly at a higher HR). Those crystalline structures require water, which explains the migration of water from gluten to starch. The crystallized rigid starch network formed during staling traps the bound water in its structure (Hemdane et al., 2017). These mechanisms lead to an increase in crumb firmness, as observed in **Fig. 1A**. The population abundance (P_{2E}) and relaxation time (T_{2E}) of the longest component (population E) that characterized the extragranular water fraction decreased significantly ($p<0.05$) for the two higher HRs whereas it did not vary for the lowest. This could be due to complete starch granule gelatinization at lower HRs, which was not achieved at higher HRs according to a calorimetric study.

4. Conclusion:

In this study, the impacts of different HRs on crumb was investigated using a miniaturized baking process (Peltier-baking system) that allows for good control of the HR and the time-temperature profile during baking. The staling kinetics were assessed based on the water mobility, starch microstructure, thermodynamic properties and mechanical properties of crumb. The ^{1}H NMR relaxation time of the five identified populations decreased with increasing HR and during staling. This could be explained by the loss of water from the gluten network, which undergoes dehydration, from the migration of water from gluten to

starch, and its incorporation in starch crystallites. In addition, baking at higher HR (40°C/min) yielded an incomplete starch gelatinization (80%) of crumb samples. In morphological ESEM observations, severe deformation and disruption were observed for most starch granules in crumbs treated at a higher HR (40°C/min). The results confirm that the firmness of bread crumb is related to the hydration of starch granules and the water trapped by AP crystals as well as the presence of AM associations that strongly affect the crumb texture. These results add useful findings to the literature and provide an important insight at industrial scale when non-CVB processes such as microwave baking are considered.

ACKNOWLEDGMENTS: This study was supported by the National Association of Technical Research of FRANCE (CIFRE thesis N° 2017/1712). The technical support of Delphine QUEVAUD is greatly appreciated.

References

Assifaoui, A., Champion, D., Chiotelli, E., Verel, A., 2006. Characterization of water mobility in biscuit dough using a low-field 1H NMR technique. Carbohydr. Polym. 64, 197–204.

Besbes, E., Jury, V., Monteau, J.Y., Le Bail, A., 2014. Effect of baking conditions and storage with crust on the moisture profile, local textural properties and staling kinetics of pan bread. LWT- Food Sci. Technol. 58, 658-66.

Besbes, E., Le Bail, A., Seetharaman, K., 2014. Effect of baking conditions on properties of starch isolated from bread crumbs: pasting properties, iodine complexing ability, and X-Ray patterns. Food Bioprocess Technol. 7, 3407–3415.

Berman, P., Levi, O.. Parmet, Y., Saunders, M., 2013. Laplace inversion of sparse representation relaxometry data using low-resolution NMR methods. Concepts Magn. Reson. Part A Bridg. Educ. Res. 42 (3), 72-88.

Bilbao-Sáinz, C., Butler, M., Weaver, T., Bent, J., 2007. Wheat starch gelatinization under microwave irradiation and conduction heating. Carbohydr. Polym. 69, 224–232.

Bosmans, G.M., Lagrain, B., Fierens, E., Delcour, J.A., 2013. The impact of baking time and bread storage temperature on bread crumb properties. Food Chem. 141, 3301–3308.

Bosmans, G.M., Lagrain, B., Ooms, N., Fierens, E., Delcour, J.A., 2014. Storage of parbaked bread affects shelf life of fully baked end product: A 1H NMR study. Food Chem. 165, 149–156.

Bredariol, P., Spatti, M., Vanin, F.M., 2019. Different baking conditions may produce breads

with similar physical qualities but unique starch gelatinization behaviour. LWT - Food Sci. Technol. 111, 737–743.

Chen, P.L., Long, Z., Ruan, R., Labuza, T.P., 1997. Nuclear magnetic resonance studies of water mobility in bread during storage. LWT - Food Sci. Technol. 30, 178–183.

Chinachoti, P., 2013. NMR dynamics properties of water in relation to thermal characteristics in bread. In: Reid, D.S. (Eds), The Properties of Water in Foods ISOPOW 6. Springer, Boston, MA, pp.139-159.

Curti, E., Bubici, S., Carini, E., Baroni, S., Vittadini, E., 2011. Water molecular dynamics during bread staling by Nuclear Magnetic Resonance. LWT - Food Sci. Technol. 44, 854–859.

Curti, E., Carini, E., Bonacini, G., Tribuzio, G., Vittadini, E., 2013. Effect of the addition of bran fractions on bread properties. J. Cereal Sci. 57, 325–332.

Curti, E., Carini, E., Cobo, M.F., Bocher, T., Vittadini, E., 2017. The use of two-dimensional NMR relaxometry in bread staling: a valuable tool. Food Chem. 237, 766–772.

Ding, L., Zhang, B., Tan, C.P., Fu, X., Huang, Q., 2019. Effects of limited moisture content and storing temperature on retrogradation of rice starch. Int. J. Biol. Macromol. 137, 1068–1075.

Engelsen, S.B., Jensen, M.K., Pedersen, H.T., Nørgaard, L., Munck, L., 2001. NMR-baking and multivariate prediction of instrumental texture parameters in bread. J. Cereal Sci. 33, 59–69.

Goesaert, H., Slade, L., Levine, H., Delcour, J.A., 2009. Amylases and bread firming – an integrated view. J. Cereal Sci. 50, 345–352. Gray, J. A., Bemiller, J.N., 2003. Bread staling: Molecular basis and control. Compr. Rev. Food Sci. Food Saf. 2, 1–21.

Gujral, H.S., Haros, M., Rosell, C.M., 2003. Starch Hydrolyzing Enzymes for Retarding the Staling of Rice Bread. Cereal Chem. 80, 750–754.

Hemdane, S., Jacobs, P.J., Bosmans, G.M., Verspreet, J., Delcour, J.A., Courtin, C.M., 2017. Study on the effects of wheat bran incorporation on water mobility and biopolymer behavior during bread making and storage using time-domain 1H NMR relaxometry. Food Chem. 236, 76–86.

Kang, X., Yu, B., Zhang, H., Sui, J., Guo, L., El-aty, A.M.A., Cui, B., 2021. The formation and *in vitro* enzymatic digestibility of starch-lipid complexes in steamed bread free from and supplemented with different fatty acids : Effect on textural and retrogradation properties during storage. Int. J. Biol. Macromol. 166, 1210–1219.

Le-Bail, A., Agrane, S., Queveau, D., 2012. Impact of the baking duration on bread staling kinetics. Food Bioprocess Technol. 5, 2323–2330.

Le-Bail, A., Boumali, K., Jury, V., Ben-Aissa, F., Zuniga, R., 2009. Impact of the baking kinetics on staling rate and mechanical properties of bread crumb and degassed bread crumb. J. Cereal. Sci. 50, 235–240.

Lee, E., Song, H., Choi, I., Lee, J., Han, J., 2020. Effects of mung bean starch / guar gum-based edible emulsion coatings on the staling and safety of rice cakes. Carbohydr. Polym. 247, 116696.

Mathias, K., Ruegg, R., Weber, C.A., Buchli, J., Durrer, L., Mûller, N., 2021. Impact of selected baking and vacuum cooling parameters on the quality of toast bread. J. Food Sci. Technol. 1-9.

Mouneim, H., Besbes, E., Jury, V., Monteau, J.Y., Le-Bail, A., 2012. Combined effects of baking conditions and bacterial α-amylases on staling kinetics of degassed and porous bread crumb. Food Bioprocess Technol. 5, 3032–3041.

Ozkoc, O.O., Sumnu, G., Sahin, S., 2009. The effects of gums on macro and micro-structure of breads baked in different ovens. Food Hydrocolloids 23, 2182–2189.

Palav, T., Seetharaman, K., 2007. Impact of microwave heating on the physico-chemical properties of a starch-water model system. Carbohydr. Polym. 67, 596–604.

Patel, B.K., Seetharaman, K., 2006. Effect of heating rate on starch granule morphology and size. Carbohydr. Polym. 65, 381–385.

Patel, B.K., Waniska, R.D., Seetharaman, K., 2005. Impact of different baking processes on bread firmness and starch properties in breadcrumb. J. Cereal. Sci. 42, 173–184.

Ribotta, P.D., Le Bail, A., 2007. Thermo-physical assessment of bread during staling. LWT - Food Sci. Technol. 40, 879–884.

Rojas, J.A., Rosell, C.M., Benedito De Barber, C., 2001. Role of maltodextrins in the staling of starch gels. Eur. Food Res. Technol. 212, 364–368.

Roman-Gutierrez, A.D., Guilbert, S., Cuq, B., 2002. Description of microstructural changes in wheat flour and flour components during hydration by using environmental scanning electron microscopy. LWT - Food Sci. Technol. 35, 730–740.

Rondeau-Mouro, C., Godfrin, C., Cambert, M., Rouillac, J., Diascorn, Y., Lucas, T., Grenier, D., 2019. Characterization of gluten-free bread crumb baked at atmospheric and reduced pressures using TD-NMR. Magn. Reson. Chem. 57, 649–660.

Sang, W., Shao, X., Jin, Z.T., 2015. Texture attributes, retrogradation properties and microbiological shelf life of instant rice cake. J. Food Process. Preserv. 39, 1832–1838.

Seyhun, N., Sumnu, G., Sahin, S., 2005. Effects of different starch types on retardation of staling of microwave-baked cakes. Food Bioprod. Process. 83, 1–5.

Seyhun, N., Sumnu, G., Sahin, S., 2003. Effects of different emulsifier types , fat contents , and gum types on retardation of staling of microwave-baked cakes. Nahrung. 47, 248-251.

Shen, Y., Chen, G., Li, Y., 2018. Bread characteristics and antioxidant activities of Maillard reaction products of white pan bread containing various sugars. LWT - Food Sci. Technol. 95, 308-315

Silverio, J., Svensson, E., Eliasson, A.C., Olofsson, G., 1996. Isothermal microcalorimetric studies starch retrogradation. J. Thermal. Anal. 47, 1178-1200.

Tao, Y., Yan, B., Fan, D., Zhang, N., Ma, S., Wang, L., Wu, Y., Wang, M., Zhao, J., Zhang, H., 2020. Structural changes of starch subjected to microwave heating: A review from the perspective of dielectric properties. Trends Food Sci. Technol. 99, 593–607.

562 Uzzan, M., Ramon, O., Kopelman, I.J., Kesselman, E., Mizrahi, S., 2007. Mechanism of
563 crumb toughening in bread-like products by microwave reheating. J. Agric. Food Chem.
564 55, 6553–6560.

565

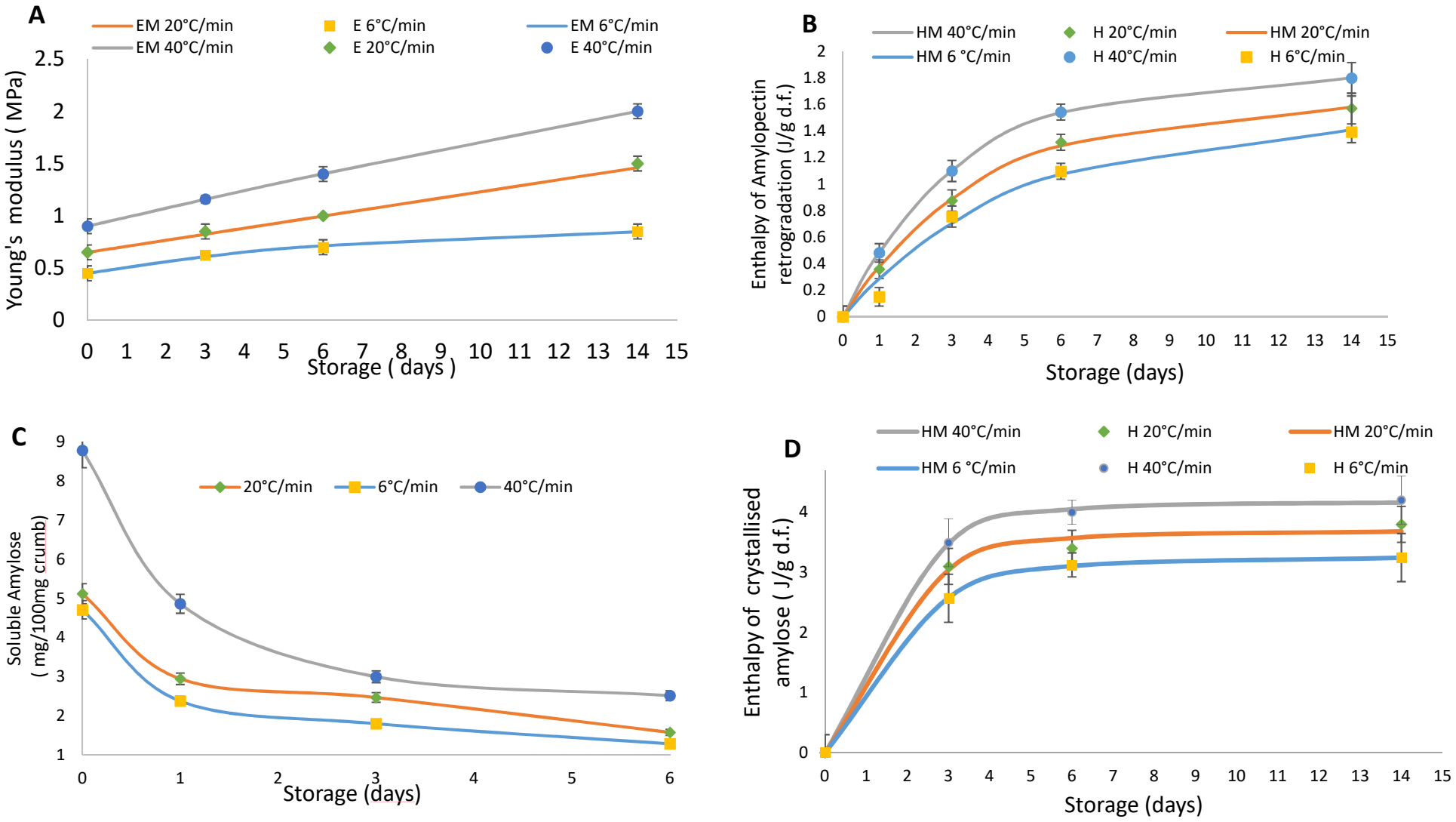

Fig. 1. Evolution of (A) crumb firmness, (B) AP recrystallization, (C) soluble AM, (D) AM crystallization in crumb baked at 6°C/min, 20°C/min and 40°C/min during storage (days) E : Experimental enthalpy, E: Experimental Young's Modulus, and HM : modeled enthalpy and EM : Modeled Young's Modulus at ■ 6°C/min, ◆ 20°C/min and ● 40°C/min.

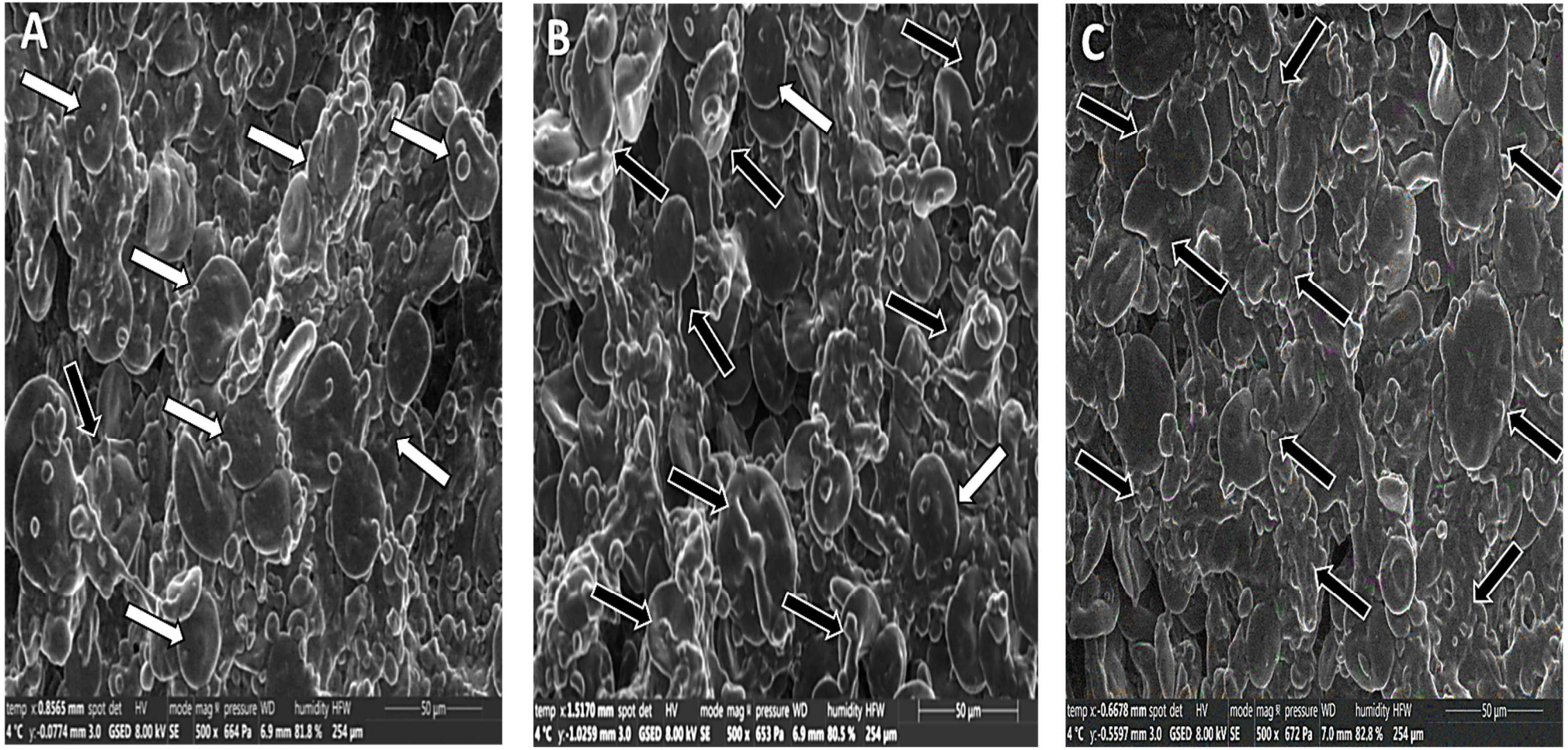

Fig.2. ESEM images for the microstructure of breadcrumbs taken at 500 × magnification baked in A) at 6°C/min, B) 20°C/min and C) 40°C/min. **The black arrows represent the destructured and deformed starch granules whilst the white arrows indicate swollen and non-deformed starch granules.

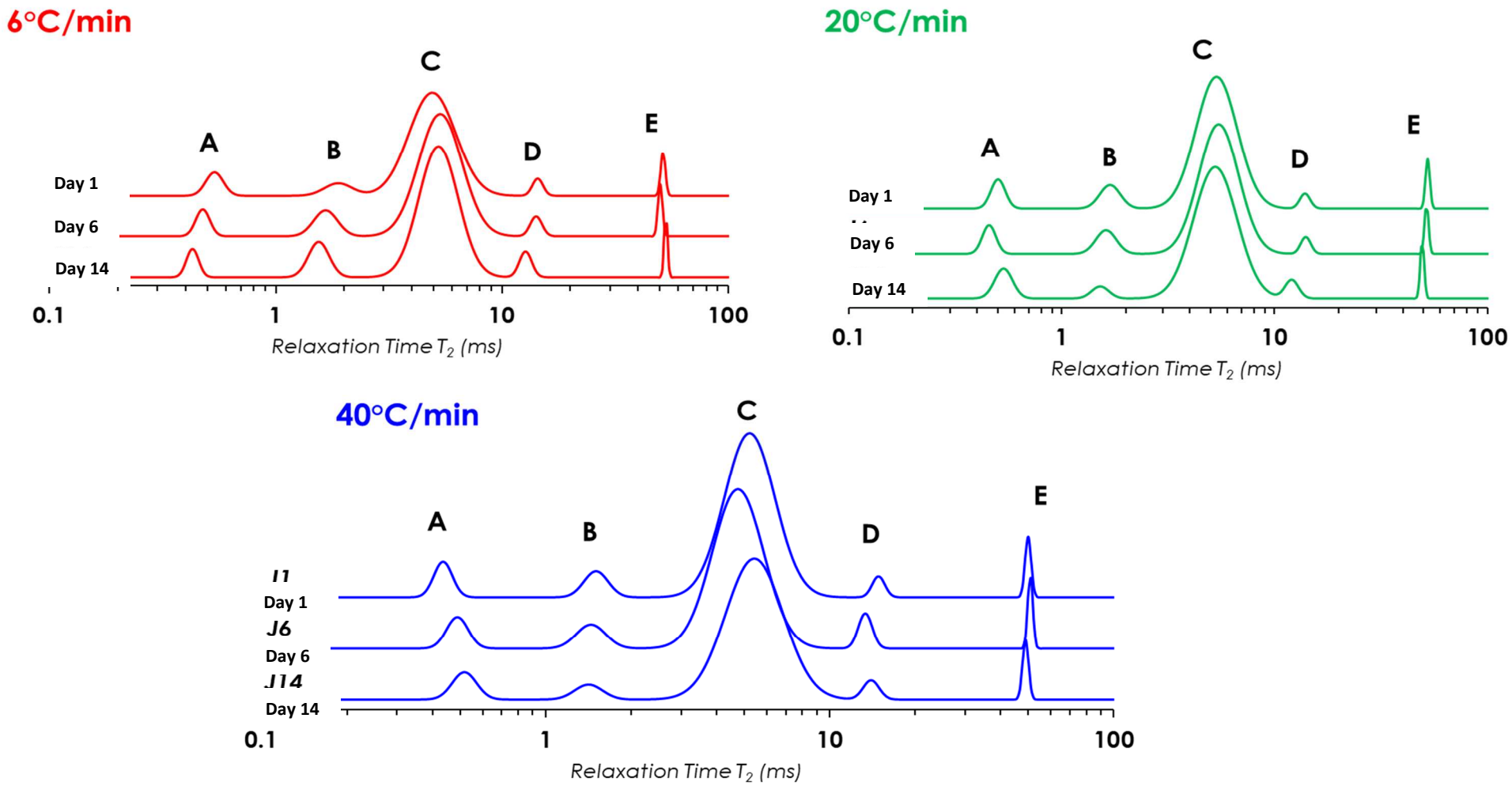

Fig. 3. Proton population distributions as a function of the T2 relaxation time of the crumb sample baked at 6°C/min, 20°C/min and 40°C/min during 1, 6, and 14 days of storage.

*The different proton population are indicated with capital letters according to their increasing mobility. Analyses were performed at 4°C.

Table 1

Effect of HR on the evolution of the melting enthalpy (E) of the retrograded amylopectin, amylose Crystallization and Young's Modulus (H) after baking and at the end of storage and on the time constant for the three-studied parameters

HR (°C/min)	Staling parameters	E0 (MPa)/ΔH0 (J/g d.f.)	$\boldsymbol{E}_{\infty}$ (MPa)/ $\Delta\boldsymbol{H}_{\infty}$ (J/g d.f.)	$\tau(days)$
6°C/ min	Young's Modulus	0.45 ± 0.05^{c}	0.85 ± 0.80^{c}	1.14 ± 0.07^{a}
	Amylopectin retrogradation	0.00 ± 0.00^{a}	1.40 ± 0.02^{b}	5.75 ± 0.02^{a}
	Amylose crystallization	0.00 ± 0.002^{a}	3.24 ± 0.03^{c}	2.00 ± 0.06^{a}
20°C/min	Young's modulus	0.65 ± 0.07^{b}	1.50 ± 0.07^{b}	0.76 ± 0.05^{b}
	Amylopectin retrogradation	0.00 ± 0.00^{a}	1.60 ± 0.06^{b}	4.28 ± 0.41^{b}
	Amylose crystallization	0.00 ± 0.004^{a}	3.69 ± 0.02^{b}	1.54 ± 0.01
40°C/min	Young's modulus	0.90 ± 0.07^{a}	2.00 ± 0.14^{a}	0.60 ± 0.02^{c}
	Amylopectin retrogradation	0.004 ± 0.001^{a}	1.90 ± 0.15^{a}	3.48 ± 0.29^{c}
	Amylose crystallization	0.002 ± 0.005^{a}	4.17 ± 0.05^{a}	1.05 ± 0.05^{c}

*Within a column, Values with the same small letter for different HR and same staling parameter are not statistically significant ($p<0.05$), ±SD

Table 2

NMR population abundance for each crumb samples baked at different HR in function of storage time (days)

HR (°C/min)	Storage time (days)	Population abundance (%)				
		P_{2a}	P_{2b}	P_{2c}	P_{2d}	P_{2e}
6°C/min	1	3.5 ± 0.02^{aB}	2.8 ± 0.04^{aA}	81.2 ± 0.01^{aB}	6.8 ± 0.02^{aA}	7.9 ± 0.008^{aA}
	6	3.3 ± 0.04^{aA}	3.0 ± 0.01^{aB}	81.0 ± 0.03^{aA}	5.8 ± 0.01^{bB}	7.1 ± 0.012^{bA}
	14	3.2 ± 0.01^{aA}	3.0 ± 0.05^{aB}	80.0 ± 0.02^{bA}	4.4 ± 0.02^{cB}	6.9 ± 0.004^{bA}
20°C/min	1	3.4 ± 0.02^{aB}	2.5 ± 0.01^{bB}	84.4 ± 0.03^{aA}	7.0 ± 0.05^{aA}	7.4 ± 0.01^{aA}
	6	3.1 ± 0.01^{aA}	3.0 ± 0.01^{aB}	80.3 ± 0.01^{bA}	4.2 ± 0.01^{bc}	6.0 ± 0.003^{bB}
	14	2.9 ± 0.03^{bB}	3.0 ± 0.02^{aB}	80.2 ± 0.02^{bA}	1.9 ± 0.02^{cc}	5.5 ± 0.006^{cB}
40°C/min	1	4.3 ± 0.04^{aA}	3.0 ± 0.01^{cA}	80.1 ± 0.01^{aB}	6.8 ± 0.01^{cA}	7.3 ± 0.008^{aA}
	6	3.1 ± 0.01^{bA}	3.9 ± 0.01^{bA}	81.5 ± 0.03^{bA}	9.3 ± 0.01^{bA}	5.8 ± 0.012^{bB}
	14	2.8 ± 0.01^{cB}	4.4 ± 0.02^{aA}	77.6 ± 0.04^{cB}	10.0 ± 0.03^{aA}	5.2 ± 0.04^{cc}

*Within a column, Values with the same small letter at different storage times of one HR and with the same capital letters at the same storage time for different HR are not statistically significant ($p<0.05$), ± SD

Heating Rate (°C/min)

Baking

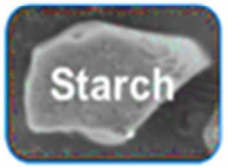

WATER MOLECULE

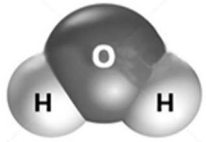

H_2O

Crumb Staling (14 days Storage)

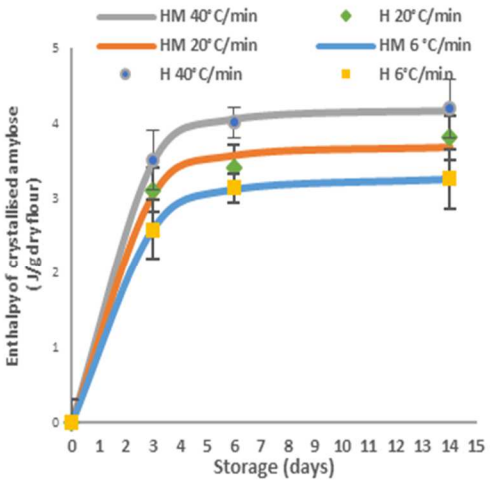

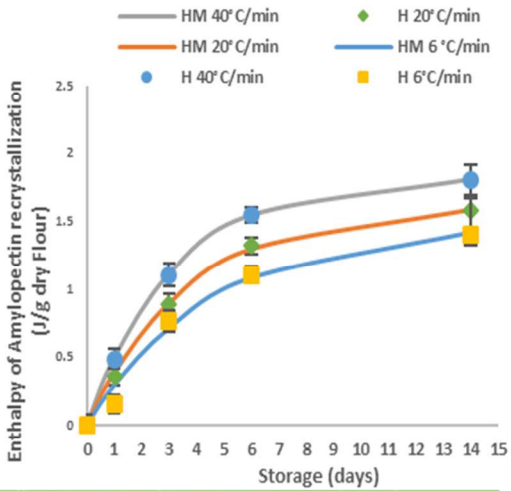

Increase of starch gelification (Amylose crystallization + Amylopectine retrogradation)

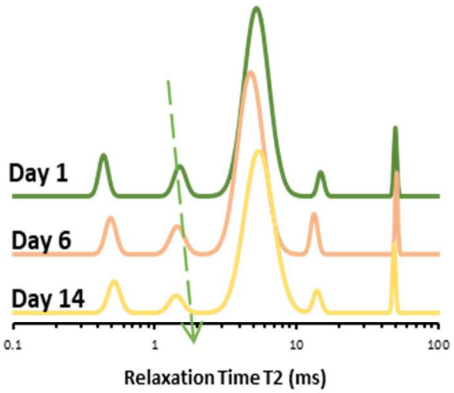

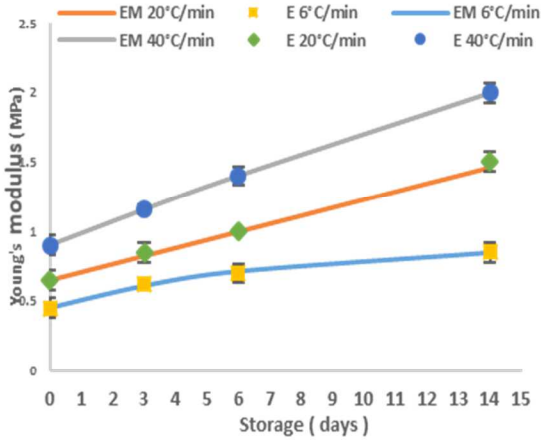

Gluten dehydration, more Bound water in starch crystallites → Increase of crumb firmness